SAND2022-1590C

ASTFE
American Society
of Thermal and Fluids Engineers

7th Thermal and Fluids Engineering Conference (TFEC)
May 16-18, 2022
Partially Online Virtual and in Las Vegas, NV Conference

TFEC-2022- 40826

AN EXPERIMENTAL AND MODELING STUDY OF OXIDATION OF HYDROGEN ISOTOPES AT TRACE CONCENTRATIONS

Randy C. Shurtz[1*], Eric N. Coker[1], Alexander L. Brown[1], Lynelle K. Takahashi[1]

[1]Sandia National Laboratories, Albuquerque, NM 87185-1135, USA

ABSTRACT

In accident scenarios involving release of tritium during handling and storage, the level of risk to human health is dominated by the extent to which radioactive tritium is oxidized to the water form (T_2O or THO). At some facilities, tritium inventories consist of very small quantities stored at sub-atmospheric pressure, which means that tritium release accident scenarios will likely produce concentrations in air that are well below the lower flammability limit. It is known that isotope effects on reaction rates should result in slower oxidation rates for heavier isotopes of hydrogen, but this effect has not previously been quantified for oxidation at concentrations well below the lower flammability limit for hydrogen. This work describes hydrogen isotope oxidation measurements in an atmospheric tube furnace reactor. These measurements consist of five concentration levels between 0.01% and 1% protium or deuterium and two residence times. Oxidation is observed to occur between about 550°C and 800°C, with higher levels of conversion achieved at lower temperatures for protium with respect to deuterium at the same volumetric inlet concentration and residence time. Computational fluid dynamics simulations of the experiments were used to customize reaction orders and Arrhenius parameters in a 1-step oxidation mechanism. The trends in the rates for protium and deuterium are extrapolated based on guidance from literature to produce kinetic rate parameters appropriate for tritium oxidation at low concentrations.

KEY WORDS: Arrhenius Oxidation Rates, Hydrogen Isotopes

1. INTRODUCTION

Tritium is a radioisotope of hydrogen that produces a low-energy beta particle upon decay and has applications in self-luminous phosphors, fusion energy production, and nuclear weapons. At U.S. Department of Energy tritium facilities, tritium is stored primarily as a diatomic gas (T_2) or as a solid hydride that can be heated to release T_2 gas. At smaller (i.e. radiological) tritium facilities, the potential flame or explosion hazard is not a major safety concern since the T_2 inventories are insufficient to sustain a flame, and gases are frequently stored at sub-atmospheric pressures. Nevertheless, T_2 to water conversion in fire environments remains a major safety concern due to radiological hazard considerations; tritiated water vapor is readily absorbed by the human body, making it 10^4 times more hazardous than the same amount of tritium uptake as T_2 gas [1, 2].

Due to the relatively high dose consequence for tritiated water on the human body, the fraction of T_2 that can convert to water vapor is an important factor in tritium safety evaluations. A report reviewing tritium safety [2] has noted that T_2 to T_2O conversions lower that 100% could (in principle) be applied for regulatory safety compliance in specific scenarios with adequate technical support. It is the aim of this paper and others by the authors [3, 4] to provide such technical support. Although extensive literature exists that examines H_2 gas combustion with high starting pressures and volumes, specific information such as molecular conversion fractions and oxidation rates under low pressures and volumes of typical concern for laboratories with tritium inventories are virtually non-existent. Even less information exists for T_2 oxidation rates due to the inherent difficulties of performing combustion experiments that generate radiologically hazardous reaction products.

*Corresponding Author: rshurtz@sandia.gov

Measured flame speeds for D_2 are slower than measured for H_2 [5-7], consistent with early observations of slower reaction rates for heavier isotopes [8]. In principle, these measurements could be used to estimate even slower flames speeds for T_2 that would be applicable to releases above the lower flammability limit. However, leaks of T_2 from a container at sub-atmospheric pressure (as is common in a radiological tritium facility) are likely to result in concentrations below the lower flammability limit, which is the regime of focus for this paper. To our knowledge, no existing literature consider oxidation rates of hydrogen isotopes in this low-concentration regime (where the non-radioactive isotopologues pose no safety hazard), especially in terms of simplified global kinetics suitable for large-scale simulations. There are a few studies of initial elementary steps in the oxidation process for H_2 and D_2 [9-12], but inferring global oxidations rates applicable at very low concentrations from these is not necessarily straightforward.

To address these critical knowledge gaps, this paper examines the non-radioactive isotopologues of diatomic hydrogen (H_2, D_2) over a range of temperature conditions in a tube reactor and their conversion to water under low concentrations in air. The experimental data from the tube reactor experiments are used to gauge how readily these isotopes react to form water vapor and determine isotopic trends. These trends are then extrapolated to produce kinetic rate parameters appropriate for tritium oxidation at low concentrations of relevance to radiological tritium facilities.

2. EXPERIMENTAL METHODS

Hydrogen gas (99.999%), deuterium gas (99.999%) and synthetic air (ultra-zero grade) were acquired from Matheson TriGas and used without purification. Gas flow rates were controlled using mass flow controllers (MFCs, Brooks). The MFCs were calibrated using a bubble-meter, and flows are reported at standard temperature and pressure.

Hydrogen isotope oxidation tests were carried out within a quartz glass cylindrical tube (internal diameter 13.5 mm, length 420 mm) in a tube furnace under a range of H_2 (D_2): air ratios, gas flow rates, and temperatures. The gas composition was monitored downstream of the quartz tube using a gas chromatograph (GC, Agilent 3000A). A cold finger was installed downstream of the quartz tube to condense out most of the water product and thereby prevent flooding of the separation column in the GC.

Fig. 1 shows a schematic representation of the tube reactor setup. Note that the hydrogen inlet was 2.5 cm inside the quartz glass tube, whereas the air flow entered the system further upstream. The hydrogen inlet tube was a piece of stainless-steel tubing (outer diameter 3.175 mm or 1/8”, inner diameter 1.75 mm), centered within the quartz. The gas within the quartz tube was maintained at atmospheric pressure, which in Albuquerque is typically 635 Torr.

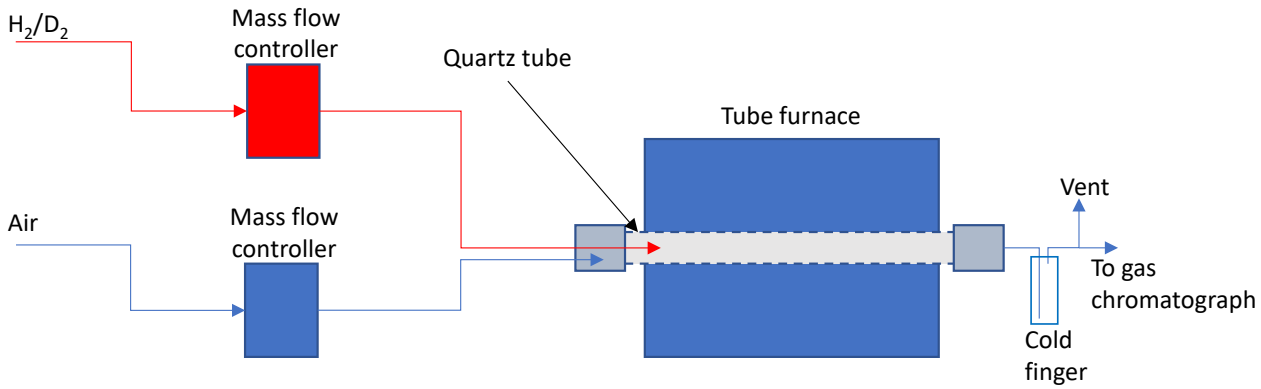

Fig. 1 Schematic representation of tube furnace reactor setup.

Once stable gas flows were achieved (as determined by GC output, typically within 10-15 mins of initiating gas flow) and the GC had been calibrated, the tube furnace was heated rapidly (stepwise) to 500°C and allowed to stabilize. No hydrogen isotope oxidation was observed at 500°C under any of the conditions used in this study, and this was used as the calibration point for the GC. The downstream cold finger was immersed in ice, and the furnace was programmed to heat at a rate of 1°C/min from 500°C to 750 or 800°C, hold for 15 minutes, and then cool at 1°C/min to 500°C. The GC drew a sample of the gas exiting the quartz tube approximately every three minutes throughout the entire experiment.

Due to differing degrees of condensation in the outlet tubing for different furnace temperatures, the experimental measurement of outlet water concentration was insufficiently reliable to use for meaningful conversion calculations. Hence, experimental conversion was calculated from residual H_2 alone (or D_2) using Equation (1):

$$X_{H_2,exp} = \frac{y_{H_2,c} - y_{H_2,f}}{y_{H_2,c}} \tag{1}$$

where X is fractional conversion of H_2 to H_2O and y is a gas-phase outlet mole fraction. The subscript "f" refers to the final or outlet concentration measurement at a given temperature and the subscript "c" specifies a concentration of H_2 or D_2 measured at the cold (500°C) furnace condition used to calibrate the GC for each set of flow conditions immediately before the oxidation experiment.

Early exploratory experiments consisted of outlet concentration measurements with several fixed temperature profiles, so temperatures at these conditions were measured along the interior wall of the quartz tube (see Fig. 2). This was done by inserting a 1/8" diameter K-type thermocouple probe through the inlet with only air flowing. Hydrogen concentrations in the oxidation experiments were low enough for thermal effects of hydrogen oxidation to be neglected for the purpose of boundary conditions (BCs). Temperatures near the ends of the tube were less accessible using this approach but were sufficiently low to be considered non-critical for the purpose of modeling the reaction rates. The shape of the temperature profiles shown in Fig. 2 near the ends of the quartz tube varies with flow rate due to the velocity dependence of convective heat transfer. Conditions with higher inlet airflow are expected to cool the inlet upstream of the heat source more efficiently, so the lower measured wall temperatures near the H_2 inlet shown in Fig. 2b at 1000 standard cubic centimeters per minute (SCCM) with respect Fig. 2a at 100 SCCM are reasonable.

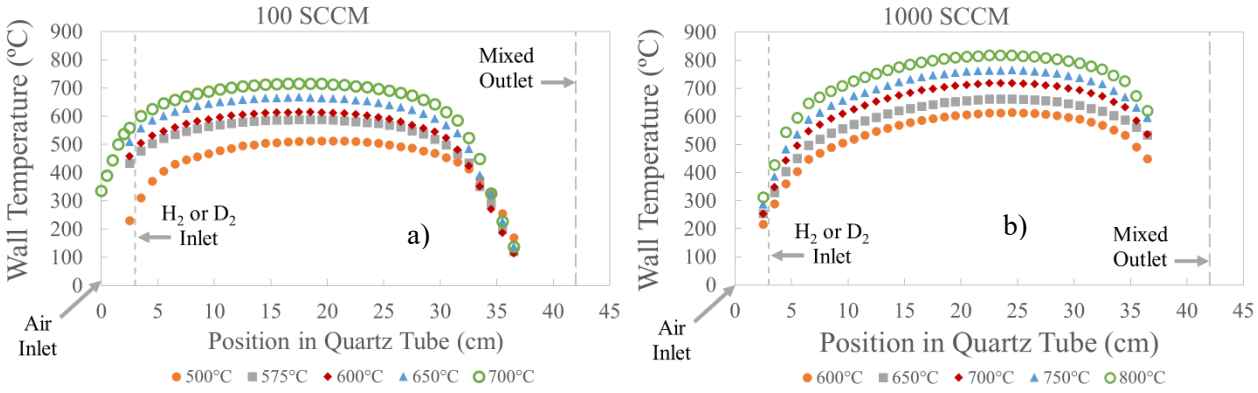

Fig. 2 Temperature profile measurements used to interpolate boundary conditions for the quartz wall.

3. MODELING APPROACH

3.1 Computational fluid dynamics modeling in SIERRA/Fuego

SIERRA/Fuego [13, 14] is a low-Mach number computational fluid dynamics (CFD) code for simulating objects in fires and is extended to support a variety of problems of interest to Sandia National Laboratories and affiliates who use the code. A major differentiating factor is that the code is a control volume finite element mechanics

(CVFEM) code rather than a more traditional control volume code. Governing equations for CFD as implemented in SIERRA/Fuego are presented in the applicable theory manual [13]. A variety of mesh elements are available to the unstructured solver. This work employed tetrahedral elements for 3-dimensional (3-D) simulations and triangular elements for 2-D simulations, as these facilitated modeling the cylinders of different sizes present in the experimental geometry.

Pre-test simulations (not shown in this work) were conducted on a 3-D tetrahedral mesh to verify that adequate mixing of hydrogen isotopes with air could be expected at a location upstream of where the temperature became sufficiently elevated for significant oxidation to occur. When post-test kinetic analysis began, a 2-D axisymmetric mesh was created to expedite iteration of parameter values (the axisymmetric simulations neglected gravity). With equivalent kinetic parameters and operating conditions, the 2-D simulations yielded nearly the same results as the 3-D simulations at the fully developed outlet (within 2% hydrogen conversion, see Fig. 3), with the computational expense reduced by a factor of 40. Fig. 3 also includes a mesh refinement study in 3-D, which likewise exhibits only minor variations in H_2 conversion when the mesh size is doubled (fine) and halved (course).

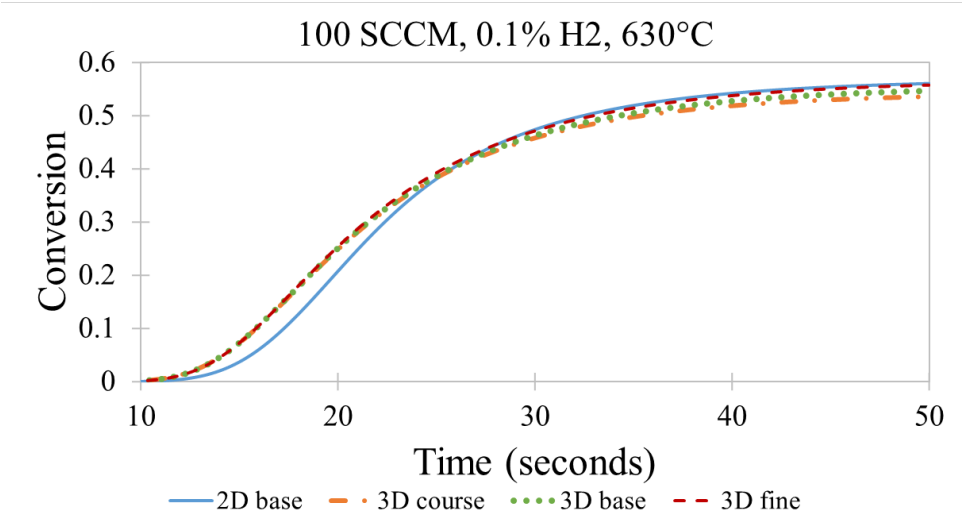

Fig. 3 H_2 conversion profiles at domain outlet with different mesh types and refinements.

Equivalent size parameters were used to generate the baseline 6934 triangular mesh elements in 2-D and the 32465 tetrahedral mesh elements in 3-D. The 2-D mesh used for the simulation results shown in this work is shown in Fig. 4, with the top view of the whole geometry mirrored to show the axis of symmetry. The magnified view of the inlet in the middle panel of Fig. 4 has two vertical edges of different sizes on the far left; the large edge is the BC for the annular air inlet and the small edge is the BC for the central hydrogen inlet tube. Both inlet BCs are specified in terms of velocity vectors, temperature (300 K or 27°C) and composition. The yellow artificial contraction in Fig. 4 was appended to the green representation of the experimental geometry. This yellow conical region was adopted to ensure that outlet concentrations sampled at the far-right edge of the green region were not influenced by spurious turbulent backflow from the simulated domain outlet. The vertical surface on the far right of the yellow region on the bottom view of Fig. 4 is the simulated domain outlet, which was defined as an open or outflow boundary condition. Any backflow occurring at this BC was defined to be air at 300 K.

The Reynolds number for the quartz tube with airflow at 100 SCCM is 10,000 at 300 K and 44,000 at 1000 K. At 1000 SCCM the Reynolds numbers increase an order of magnitude to 100,000 at 300 K and 440,000 at 1000 K. These Reynolds numbers are all well above 2300, which indicates that the experiments were all above the expected transition from the laminar to turbulent regime for interior pipe flow. However, turbulence is not expected to strongly impact the measurements and simulations of kinetics rates with this geometry. If anything, turbulence improves the kinetic measurements by ensuring radially uniform heating of the gas mixture and efficient mixing of H_2 or D_2 with air prior to achieving temperatures high enough for oxidation to occur. The gas temperatures also

cool uniformly under the influence of turbulence after exiting the heated zone. Turbulence was modeled using settings for a hybrid LES/RANS technique as per [4] in both 3-D and 2-D. These simulations are likely under-resolved in terms of turbulence, but in this simple geometry the kinetics are likely more dependent on the temperature profile than the fluid dynamics.

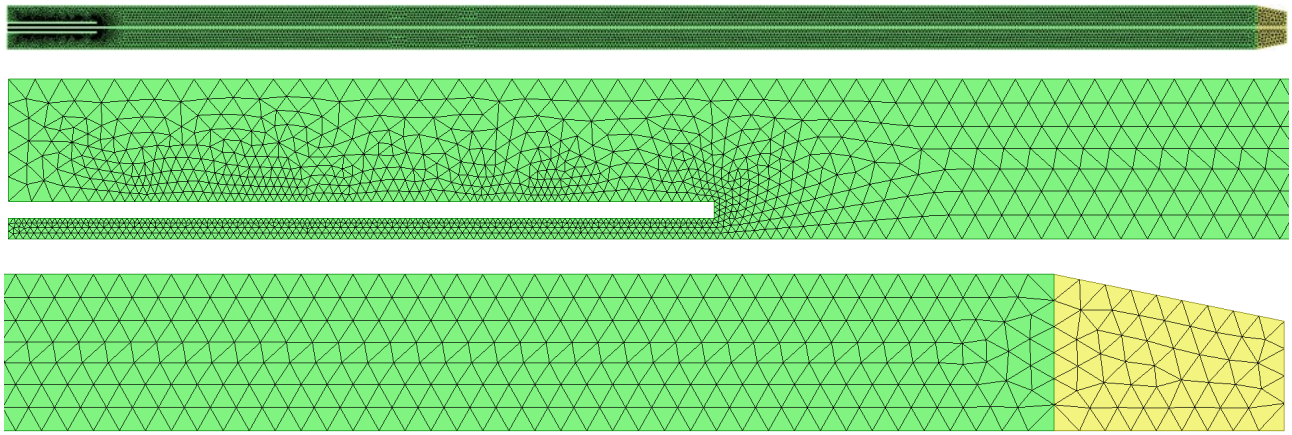

Fig. 4 Mesh used to model the hydrogen and deuterium oxidation experiments. Top view: full 2-D mesh. Middle view: inlet mesh with central hydrogen inlet and annular air inlet at left. Bottom view: outlet mesh with artificial contraction to 70% diameter over 1 cm excess length.

3.2 Kinetic modeling in SIERRA/Fuego

SIERRA/Fuego includes a capability to model user-defined reactions. Hence, Fuego simulations with the geometry in Fig. 4 accounted for flow, mixing, heating, reaction (water formation) and cooling. Temperature-dependent properties of hydrogen isotopes selected for this work are described in another paper [3]. The modeling parameters for kinetic rates were manually optimized within the CFD code. A global hydrogen oxidation mechanism from Marinov et al. (1995) [15] was initially selected for this work:

$$r_{global} = Aexp\left(-\frac{E}{RT}\right)[H_2]^{n_H}[O_2]^{n_O} \quad (2)$$

The default reaction orders of $n_H = 1.0$ and $n_O = 0.5$ specified in this equation are consistent with the stoichiometry of the global oxidation reaction ($H_2 + ½\ O_2 \rightarrow H_2O$). We have adapted the originally reported rate constants for this reaction to units required by Fuego with concentrations in mol/m^3 (indicated by square brackets) [4]. The originally reported Arrhenius parameters and reaction orders for Equation (2) were calibrated to flame speed data [15], but the regime of interest for this work corresponds to sub-flammable hydrogen concentrations (far below 4% in air at atmospheric pressure) [16, 17].

The pre-test simulations are not shown in this work, but the exercise revealed that the initial kinetic parameters [4, 15] caused simulated oxidation of hydrogen to occur at temperatures ~250°C lower than the measurements. The pre-test simulation results also indicated that a small mixing benefit could be expected from centering the hydrogen injection tube radially within the quartz reaction tube. The global reaction model represented by Equation (2) does not apply directly to all regimes because it omits intermediate species from elementary reaction steps. Therefore, it was necessary to adjust the hydrogen reaction order and the Arrhenius parameters to match our measurements of hydrogen and deuterium oxidation at low concentrations as described in the Results and Discussion.

Wall temperature profile BCs were taken directly from the measurements in Fig. 2. In some cases, these temperature profiles were linearly interpolated to achieve convenient spacing in terms of the measured conversion. Different extrapolation methods were selected to yield physically reasonable behavior near the ends of the quartz tube with different flow rates based on careful consideration of the measurements shown in Fig. 2. Temperatures near the outlet of the quartz tube with an inlet air flowrate of 100 SCCM were extrapolated

using exponential decay from the semi-logarithmic slope of the last two measured points towards an asymptotic limit of 25°C. Measurements for the temperature profile at 700°C were taken close to the inlet (upstream of the heated zone) at an air flowrate of 100 SCCM, as shown Fig. 5a. A linear slope of temperature versus position was defined from these measurements and applied to extrapolate the wall temperature towards the quartz inlet for the other profiles having the same flow rate. The left panel of Fig. 2 shows that the first measurement was taken at 2.5 cm for profiles other than 700°C at 100 SCCM. For conditions with an air inlet flowrate of 1000 SCCM the measured slopes from the two points nearest the inlet were used to extrapolate the inlet temperatures for the same profile, as shown in Fig. 5b. The same inlet slope was multiplied by -1 and used to extrapolate the outlet, with a limiter to prevent extrapolations below 25°C from occurring.

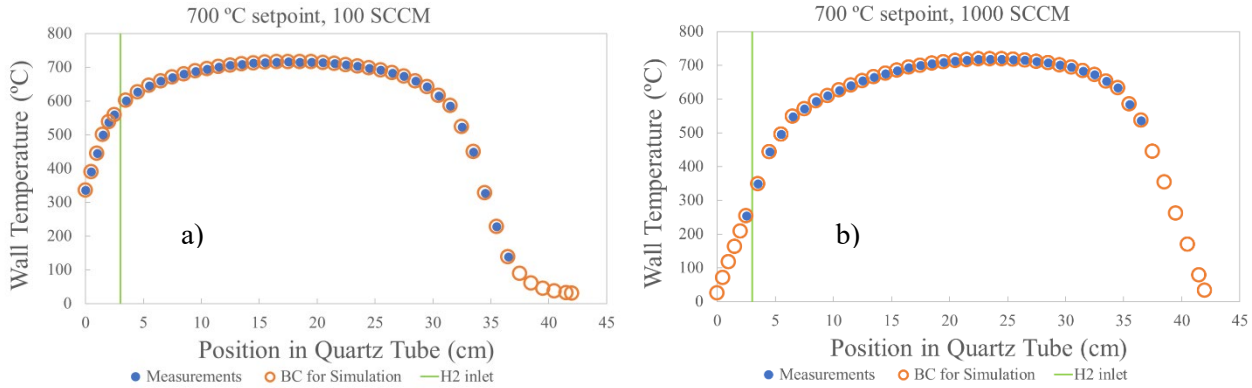

Fig. 5 Representative temperature profile measurements with boundary condition (BC) extrapolations.

The furnace control temperatures are near the plateau temperatures shown in Fig. 2 at the center of the quartz tube; these control temperatures are used to compare fractional hydrogen conversions from the simulations with respect to the measurements. This choice of reference temperatures for the non-isothermal reaction tube is consistent with the furnace temperatures supplied with the concentration measurements, which exhibited only minimal hysteresis. The conversion from the simulations is derived from both the hydrogen (H_2 or D_2) and water (H_2O or D_2O) concentrations at the simulated domain outlet (before the artificial conical contraction on the bottom right of Fig. 4) using Equation (3):

$$X_{H_2,sim} = \frac{y_{H_2O,f}}{y_{H_2,f} + y_{H_2O,f}} \tag{3}$$

where y is an outlet mole fraction at the final simulation time, which was typically 50 seconds at 100 SCCM and 20 seconds at 1000 SCCM to achieve a steady-stated condition.

4. RESULTS AND DISCUSSION

4.1 Experimental Results

The increasing and decreasing temperature scans yielded only minor hysteresis in the measured conversion of hydrogen isotopes shown in Fig. 6. This indicates that the temperature scan rate was slow enough to approximate thermal equilibrium, comparable to the static conditions measured in Fig. 2. Fig. 6a shows that the H_2 detection limit for the gas chromatograph (GC) was reached for 0.025% H_2 with 1000 SCCM air at about 95% conversion and again for 0.01% H_2 with 1000 SCCM air at about 75% conversion. As the H_2 detection limit is reached, the apparent conversion jumps to 100%. It is not surprising that these two series of measurements operating near the detection limit have the worst hysteresis, as illustrated by the arrows in Fig. 6a.

Fig. 6 shows that oxidation usually occurs at lower temperatures for H_2 than it does for D_2 with the same molar inlet concentration, which is consistent with theoretical expectations and historical observations of faster reaction rates for lighter isotopologues [18]. The exception to this trend shown in Fig. 6c and Fig. 6d occurs with both airflow rates for the lowest hydrogen or deuterium flow rates. The calibrations of the mass flow controllers and the GC are expected to be applicable for these data, but uncertainties for both flow and concentration

measurements are expected to be maximized at the lowest flow rates. At this point, experimental factors cannot be ruled out as a cause for apparent H_2 oxidation rates that are similar to or lower than D_2 oxidation rates at the lowest flow rate; follow-up investigations of this effect at low concentrations are recommended.

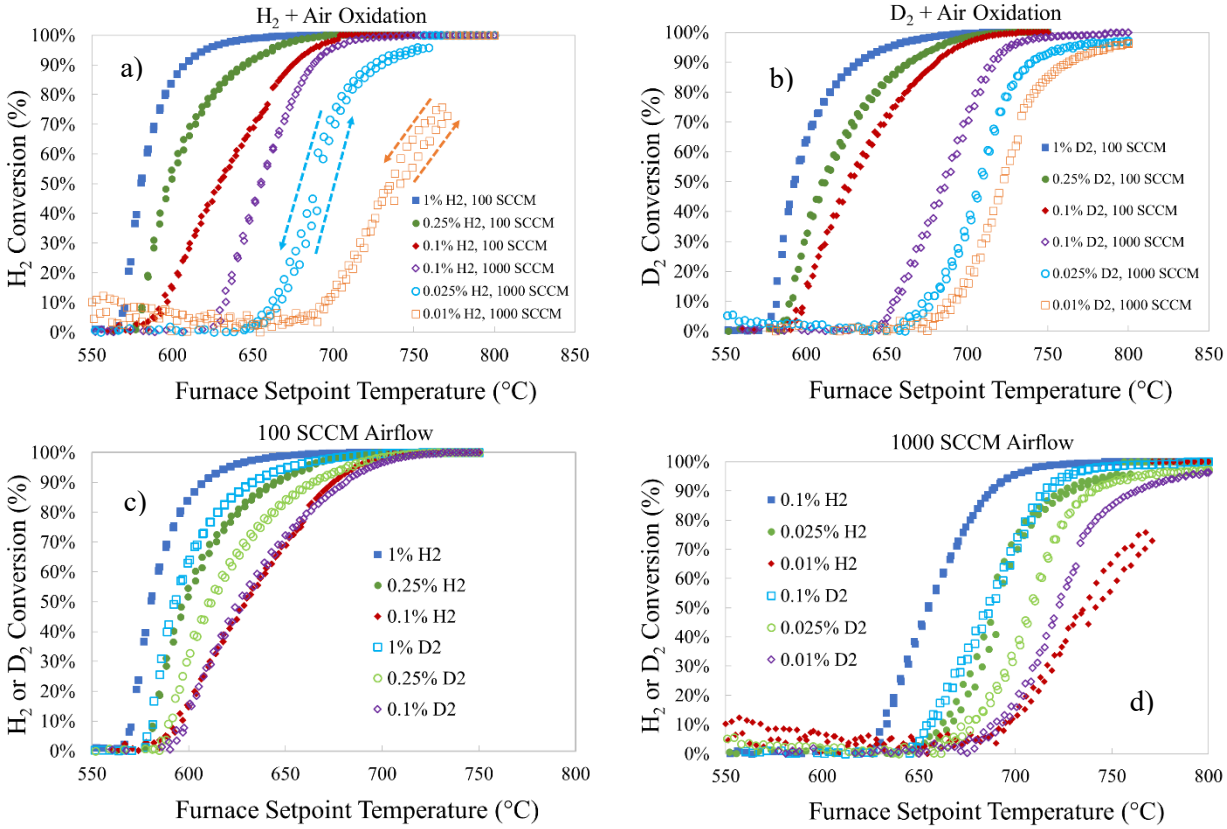

Fig. 6 Conversion of H_2 and D_2 in the tube furnace reactor; a) H_2 oxidation, b) D_2 oxidation, and both isotopes with c) 100 SCCM airflow (long residence time), and d) 1000 SCCM airflow (short residence time).

4.1 Kinetic Modeling Results Compared to Experiments

Several parameter adjustments were required for the kinetic model in Equation (2) to represent the data in Fig. 6. The kinetic parameter adjustments for this work were done manually, so the recommended parameters constitute a "visual fit" of the data rather than a statistical fit. This approach was taken to simplify the workflow, as automated optimization of parameters is tedious to set up and prone to errors when the objective function depends on the output of CFD simulations. The manual approach was deemed sufficiently accurate for the intended safety assessment applications, especially given the simplicity of the global reaction model in Equation (2) and the noise in the measurements. Equation (2) is a global mechanism that omits details inherent in the underlying elementary reaction steps. Therefore, it is too simple to predict all features in the conversion profiles over the full range of possible experimental conditions.

It was found that manual parameter adjustment was most efficient with the following order of operations. First, the activation energy E was adjusted, followed by the hydrogen reaction order n_H, with intermediate and final updates to the pre-exponential factor A as needed to ensure a good match of the target data. The default oxygen reaction order of $n_O = 0.5$ was not changed because no measurements with varying oxygen concentration were made. Oxygen concentration is not expected to vary much in applications of interest for this kinetic study, so the default oxygen reaction order is probably adequate. For brevity, the figures in this section only show simulation results with the finalized parameters, which are listed below the original values [4, 15] in Table 1.

Fig. 6 highlights measurements with hydrogen and deuterium concentrations of 0.1% with two rates of airflow. The differences in residence time are expected to be the principal cause of this behavior, and the activation energy

E is the single parameter in Equation (2) that scales residence time effects. Increasing the activation energy for the simulation of the tube reactor increases the effect of residence time (greater temperature differences for onset of oxidation) and makes conversion happen more rapidly after onset (steeper conversion versus temperature). It was also apparent from the slopes of the conversion curves that activation energies much larger than the published value of 17,600 K [4, 15] would be required. It is not surprising that the activation energies would differ, because the published value was derived from a flaming regime with much higher fuel concentrations. The activation energy and pre-exponential factors were adjusted manually until the simulated conversions were all in agreement with measured conversions in the range of 5% and 20%; this was the definition used to match the onset behavior.

Table 1 Kinetic parameters for Equation (2) for oxidation of trace concentrations of molecular hydrogen. Tritium pre-exponential factor is extrapolated from the other isotopes via Equation (4).

Isotope	Molecular Mass (g/mol)	A	E/R (K)	n_H
H_2 (protium, original [4, 15])	2.016	1.77×10^{10} $m^{1.5}/mol^{0.5}/s$	17,600	1.0
H_2 (protium, this work)	2.016	8.0×10^{24} $m^{4.5}/mol^{1.5}/s$	50,000	2.0
D_2 (deuterium, this work)	4.028	4.0×10^{24} $m^{4.5}/mol^{1.5}/s$	50,000	2.0
T_2 (tritium, extrapolated)	6.032	2.9×10^{24} $m^{4.5}/mol^{1.5}/s$	50,000	2.0

Fig. 7 shows simulation results assuming *E/R* is 50,000 K, suggesting that increasing E/R with respect to the literature value provides an acceptable match of oxidation onset in the H_2 and D_2 conversion data at 0.1% inlet concentration in air with different residence times. Fig. 7 and Fig. 8 show that the simulations and measurements are in better agreement for D_2 compared to H_2. Literature suggests that in cases where differences in activation energy exist for different isotopes, higher activation energies should be expected for the heavier isotopologues [18]. However, inspection of Fig. 7 and Fig. 8 (a and b) indicates that using a lower activation energy for H_2 in Equation (2) would make the kinetic model representation of the measurements worse because the simulated conversion curves for H_2 would become less steep and the separation in terms of temperature between the two residence times would be reduced. Likewise, it does not appear that a significant benefit would be gained by modeling D_2 with a higher activation energy, as the simulated steepness for most conditions and temperature separation of the conversion curves with different residence times are already comparable to the measurements. Therefore, the same activation energy was applied for the global oxidation reaction of all hydrogen isotopes at low concentrations (see Table 1).

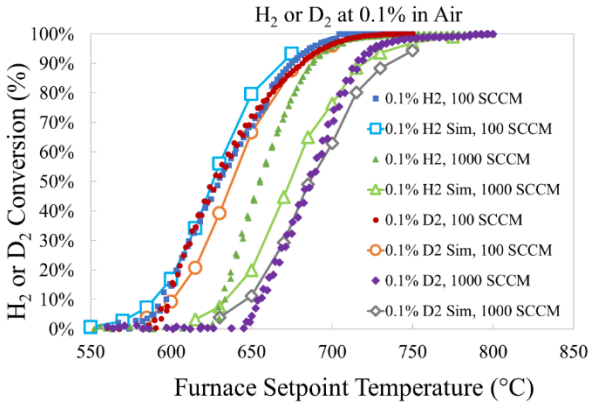

Fig. 7 Simulated and experimental conversion of H_2 and D_2 at 0.1% in air

As noted with respect to the raw measurements in connection with Fig. 6, the conversion curves for 0.1% H_2 with 100 SCCM and 0.01 H_2 with 1000 SCCM (with the lowest flow rate) could be expected to occur at slightly lower temperatures based on the comparison to the analogous D_2 oxidation measurements. If the pre-exponential factor for H_2 were increased to produce such an effect (shifting the open orange diamonds in Fig. 8 to the left), the simulations with higher concentrations in panels a and b of Fig. 8 (open blue squares and green circles) would also shift to the left. Several replicates and/or different measurement approaches would be required to demonstrate the presence of an error for the measurements represented by the solid red diamonds in panels a

and b of Fig. 8. Despite the potential improvement compared to experiments at moderate levels of conversion, the current lack of corroborating data precludes justifying an increase in the modeled H_2 rates at present.

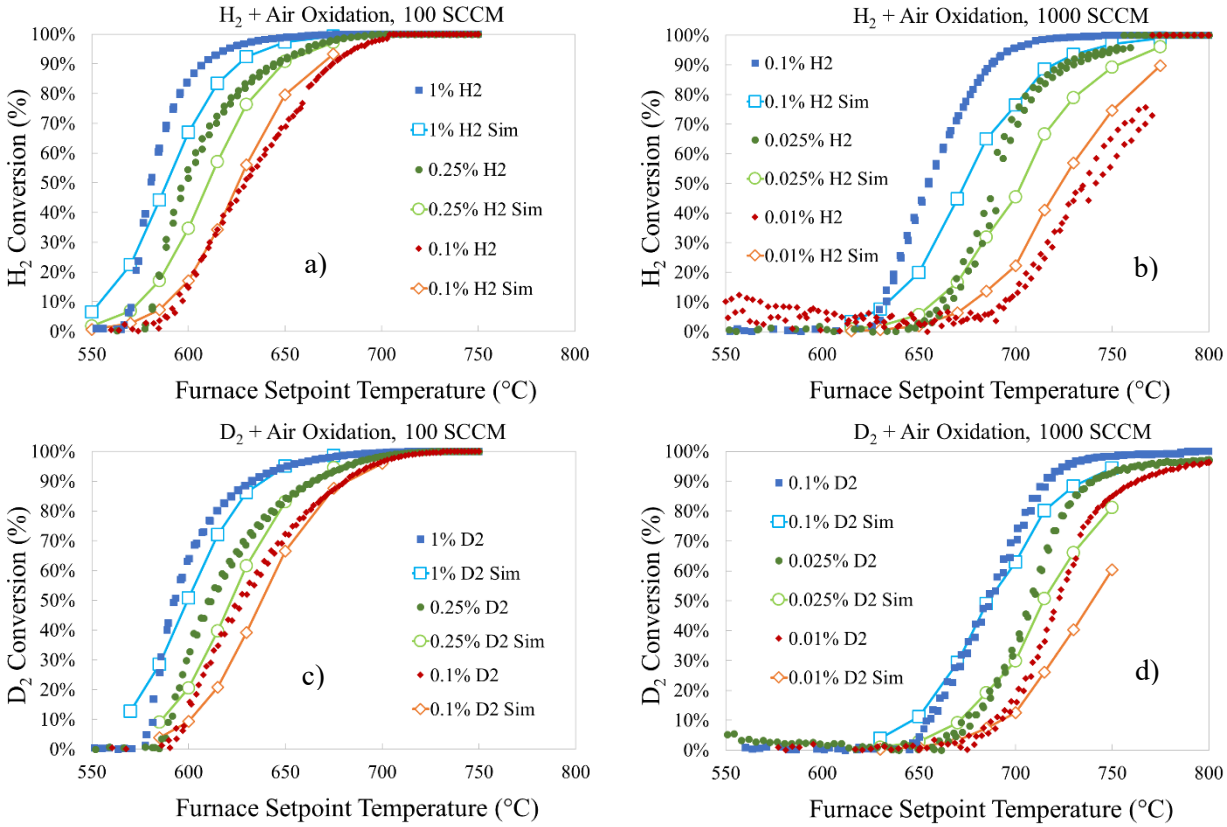

Fig. 8 Simulated and experimental conversion of H_2 and D_2 with two residence times (airflow rates).

Fig. 8 shows that the simulations compare favorably to the measurements from D_2 and H_2, especially in terms of the fundamental trends. Attempts to model oxidation with the default hydrogen reaction order of $n_H = 1.0$ disallowed any differences between the three simulations shown within each panel of Fig. 8 (open blue squares, green circles, and orange diamonds). This makes sense for a first-order reaction because increasing the flow rate of the limiting reactant by an arbitrary factor with an identical temperature history will cause the reaction rate to increase by the same factor; the higher average reaction rates cancel with the higher initial reactant concentration when the data are normalized as fractional conversions. Parameter scoping exercises indicate that the optimal reaction order should be near $n_H = 2.0$ for both D_2 and H_2. Values of n_H closer to 3.0 yield too much separation between conversion curves. An integer value for n_H is preferred, as it produces simpler units for the pre-exponential factor, and the measurement uncertainty combined with the oversimplified form of Equation (2) with respect to the constituent elementary reaction steps preclude achieving a fit much better than shown in Fig. 8 with non-integer values of n_H. The optimal value for the reaction order is dependent on the choice of the activation energy, so simulated curves with imperfect conversion slopes can only exhibit accurate concentration scaling in a narrow range of temperatures. The reaction order of $n_H = 2.0$ performs best at the temperature in each panel of Fig. 8 where the lowest conversions (open orange diamonds) are 10% or lower.

4.3 Kinetic Modeling of Tritium Oxidation

The pre-exponential factor shifts the simulated conversion curves left and right in terms of the plots shown in this paper without much change in the shape or spacing between the various curves (in terms of either the temperature or conversion axes). With the same activation energy and reaction order, increasing the rate of H_2 oxidation by a factor of 2 with respect to the optimized D_2 parameters yielded the best simulated results in Fig. 7 and Fig. 8. This approach simplifies scaling the kinetic rates for T_2, which is the objective driving this work.

Arrhenius rate constants are defined as $k = Aexp(-E/RT)$. A relationship for isotopic pairs of Arrhenius rate constants may be derived from kinetic (collision) theory of gases, where molecular velocities are inversely related to the square root of molecular weight. This relationship is given by [18, 19]:

$$\left(\frac{k_H}{k_T}\right) = \left(\frac{k_H}{k_D}\right)^{1.44} \tag{4}$$

where the subscripts H, D and T refer to normal hydrogen (protium), deuterium, and tritium. The exponent of 1.44 is defined using the following function of atomic masses [18, 19]:

$$\frac{1-\sqrt{\frac{m_H}{m_T}}}{1-\sqrt{\frac{m_H}{m_D}}} = 1.44 \tag{5}$$

Equation (4) neglects quantum effects such as tunneling, which may become non-negligible at the high temperatures investigated in this work. However, Equation (4) has been successful in describing experimental trends over a very broad range of conditions [18, 20, 21]. Equation (4) is expected to capture the most important aspects of the isotopic trend in reaction rates and is recommended as the best available method to scale the experimentally-derived pre-exponential factors in Table 1 from protium and deuterium to produce the recommended value for the tritium pre-exponential factor.

If future measurements indicate higher H_2 oxidation rates are appropriate at low concentrations, as discussed in connection with Fig. 8, then the tritium pre-exponential factor in Table 1 would be reduced in accordance with Equation (4). In other words, the most probable bias direction for experimentally derived oxidation rate parameters for H_2 and D_2 would cause modeled tritium oxidation rates to be higher than reality. If the currently recommended parameters in Table 1 result in modeling excess conversion of tritium to water, this would result in a degree of conservatism when modeling hazards associated with a tritium leak scenario. With or without a small experimental bias, such modeling assessments are expected to be more realistic than the current assumption of 100% conversion [1, 4].

6. CONCLUSIONS

This work reports oxidation measurements for H_2 and D_2 at sub-flammable concentrations in a tube furnace, with five concentrations from 0.01% to 1% by volume in air. Oxidation to the water form (H_2O or D_2O, respectively) occurred between 550°C and 800°C, and the rates of protium conversion exceeded the deuterium oxidation rates for most experimental conditions. These experimental trends indicate that tritium should have oxidation rates lower than the measured deuterium rates reported in this study. Furthermore, the hydrogen oxidation rates reported in this work were significantly slower than predicted by a global 1-step reaction model that was originally developed from high-concentration measurements in the flammable regime [15]; H_2 in pre-test simulations of the experiments oxidized between 350°C and 500°C.

These results have safety implications for tritium, as the hazard level for a release scenario is largely determined by the fraction of released tritium that is converted to the more hazardous water form (T_2O or THO). The low measured oxidation rates for H_2 and D_2 and the expected reduction in oxidation rates for T_2 with respect to the lighter hydrogen isotopes both imply that a substantial fraction of tritium released in a credible low-concentration scenario is likely to remain unoxidized in the vicinity of a heat source such as a fire [4].

Rate parameters for a global 1-step hydrogen oxidation reaction [15] were adapted in this work to model the experimentally measured conversions, using a common apparent reaction order and activation energy for H_2 and D_2 in the low-concentration regime. The same reaction order and activation energy are recommended for T_2 oxidation, while the tritium pre-exponential factor was extrapolated from the experimentally derived trends of protium and deuterium oxidation. The global rate expression with the parameters recommended in this study

are intended to facilitate comparisons to other data sources and to provide an alternative means to evaluate the hazards of tritium release scenarios with respect to the typical regulatory assumption of 100% oxidation [1].

ACKNOWLEDGMENT

Sandia National Laboratories is a multi-mission laboratory managed and operated by National Technology and Engineering Solutions of Sandia, LLC., a wholly owned subsidiary of Honeywell International, Inc., for the U.S. Department of Energy's National Nuclear Security Administration under contract DE-NA-0003525. This paper describes objective technical results and analysis. Any subjective views or opinions that might be expressed in the paper do not necessarily represent the views of the U.S. Department of Energy or the United States Government.

REFERENCES

[1] *Tritium Handling and Safe Storage*, DOE-STD-1129-2015, Washington, D.C., (2015).
[2] J. Mishima and C. M. Steele, *Oxidation of Tritium Gas Under Accident and Transport Conditions*, LA-UR-02-3803, (July 2002).
[3] R. C. Shurtz, A. L. Brown, L. K. Takahashi, M. R. Kesterson, and J. E. Laurinat, "A Suite of Thermodynamic and Transport Properties for Computational Simulations with Hydrogen Isotopes," presented at the 12th US National Combustion Institute Meeting, Virtual Meeting Hosted by Texas A&M and CSSCI, (May 24-26, 2021), Paper 128FR-0224.
[4] A. L. Brown, R. C. Shurtz, L. K. Takahashi, M. R. Kesterson, and J. E. Laurinat, "A Computational Scenario Based Assessment of Hydrogen Isotope (3H) Fire Safety," presented at the 12th US National Combustion Institute Meeting, Virtual Meeting Hosted by Texas A&M and CSSCI, (May 24-26, 2021), 128FR-0216.
[5] G. W. Koroll and R. K. Kumar, "Isotope effects on the combustion properties of deuterium and hydrogen," *Combustion and Flame,* vol. 84, no. 1, pp. 154-159, (1991), doi: https://doi.org/10.1016/0010-2180(91)90044-C.
[6] P. Gray, S. Holland, and D. B. Smith, "The effect of isotopic substitution on the flame speeds of hydrogen-oxygen and hydrogen-nitrous oxide flames," *Combustion and Flame,* vol. 14, no. 3, pp. 361-374, (1970), doi: https://doi.org/10.1016/S0010-2180(70)80050-5.
[7] P. Gray and D. B. Smith, "Isotope effects on flame speeds for hydrogen and deuterium," *Chemical Communications (London),* 10.1039/C19670000146 no. 4, pp. 146-148, (1967), doi: 10.1039/C19670000146.
[8] C. N. Hinshelwood, A. T. Williamson, and J. H. Wolfenden, "The Reaction Between Oxygen and the Heavier Isotope of Hydrogen," *Proceedings of the Royal Society of London. Series A, Mathematical and Physical Sciences,* vol. 147, no. 860, pp. 48-57, (1934). [Online]. Available: http://www.jstor.org/stable/2935460.
[9] A. A. Westenberg and N. de Haas, "Atom−Molecule Kinetics Using ESR Detection. III. Results for O+D2→OD+D and Theoretical Comparison with O+H2→OH+H," *The Journal of Chemical Physics,* vol. 47, no. 10, pp. 4241-4246, (1967), doi: 10.1063/1.1701606.
[10] J. V. Michael, "Rate constants for the reaction O+D2→OD+D by the flash photolysis‐shock tube technique over the temperature range 825‐2487 K: The H2 to D2 isotope effect," *The Journal of Chemical Physics,* vol. 90, no. 1, pp. 189-198, (1989), doi: 10.1063/1.456513.
[11] P. Marshall and A. Fontijn, "HTP kinetics studies of the reactions of O(2 3PJ) atoms with H2 and D2 over wide temperature ranges," *The Journal of Chemical Physics,* vol. 87, no. 12, pp. 6988-6994, (1987), doi: 10.1063/1.453395.
[12] K. M. Pamidimukkala and G. B. Skinner, "Resonance absorption measurements of atom concentrations in reacting gas mixtures. VIII. Rate constants for O+H2→OH+H and O+D2→OD+D from measurements of O atoms in oxidation of H2 and D2 by N2O," *The Journal of Chemical Physics,* vol. 76, no. 1, pp. 311-315, (1982), doi: 10.1063/1.442779.
[13] SIERRA Thermal/Fluid Development Team, *SIERRA Low Mach Module: Fuego Theory Manual - Version 4.58*, Sandia National Laboratories, SAND2020-11535, (October 2020).
[14] SIERRA Thermal/Fluid Development Team, *SIERRA Low Mach Module: Fuego User Manual - Version 4.58*, Sandia National Laboratories, SAND2020-11536, (October 2020).
[15] N. M. Marinov, C. K. Westbrook, and W. J. Pitz, "Detailed and Global Chemical Kinetics Model for Hydrogen," presented at the 8th International Symposium on Transport Properties, San Francisco, California, United States, (March 1995). Available: https://www.osti.gov/servlets/purl/90098.
[16] M. Hertzberg, "Flammability limits and pressure development in H2-air mixtures," presented at the Workshop on the Impact of Hydrogen on Water Reactor Safety, Albuquerque, NM, United States, pp. 13-67, (September, 1981), NUREG/CR--2017-Vol3. Available: http://inis.iaea.org/search/search.aspx?orig_q=RN:15046472.
[17] F. J. Benz and P. L. Boucher, "Flammability characteristics of hydrogen/oxygen/nitrogen mixtures at reduced pressures," presented at the Workshop on the Impact of Hydrogen Water Reactor Safety, Albuquerque, NM, United States, pp. 137-169, (September, 1981), NUREG/CR--2017-Vol3. Available: http://inis.iaea.org/search/search.aspx?orig_q=RN:15047089.
[18] L. Melander and W. H. Saunders, *Reaction rates of isotopic molecules*. New York: Wiley, pp. 28-29, (1980).
[19] C. G. Swain, E. C. Stivers, J. F. Reuwer, and L. J. Schaad, "Use of Hydrogen Isotope Effects to Identify the Attacking Nucleophile in the Enolization of Ketones Catalyzed by Acetic Acid1-3," *Journal of the American Chemical Society,* vol. 80, no. 21, pp. 5885-5893, (1958), doi: 10.1021/ja01554a077.

[20] E. S. Lewis and J. K. Robinson, "The influence of tunneling on the relation between tritium and deuterium isotope effects. The exchange of 2-nitropropane-2-t," *Journal of the American Chemical Society,* vol. 90, no. 16, pp. 4337-4344, (1968), doi: 10.1021/ja01018a025.

[21] M. J. Stern and R. E. Weston, "Phenomenological manifestations of quantum‐mechanical tunneling. III. Effect on relative tritium‐deuterium kinetic isotope effects," *The Journal of Chemical Physics,* vol. 60, no. 7, pp. 2815-2821, (1974), doi: 10.1063/1.1681449.